Chin. J. Astron. Astrophys. Vol. 6 (2006), No. 4, 387–395
(*http://www.chjaa.org*)

Chinese Journal of
Astronomy and
Astrophysics

On the Large-Scale Structure of the Universe as given by the Voronoi Diagrams

L. Zaninetti

Dipartimento di Fisica Generale, Via Pietro Giuria 1 10125 Torino, Italy; *zaninetti@ph.unito.it*

Received 2005 November 17; accepted 2006 February 14

Abstract The size distributions of 2D and 3D Voronoi cells and of cells of $V_p(2,3)$,—2D cut of 3D Voronoi diagram—are explored, with the single-parameter (re-scaled) gamma distribution playing a central role in the analytical fitting. Observational evidence for a cellular universe is briefly reviewed. A simulated $V_p(2,3)$ map with galaxies lying on the cell boundaries is constructed to compare, as regards general appearance, with the observed CfA map of galaxies and voids, the parameters of the simulation being so chosen as to reproduce the largest observed void size.

Key words: surveys — galaxies: clusters: general — (cosmology:) large-scale structure of Universe

1 INTRODUCTION

Applications of the Voronoi diagram (see Voronoi 1980) in astrophysics started with Kiang (1966) where the size distribution of 1D Voronoi cells given by random seeds was theoretically deduced in a rigorous way. Kiang (1966) also derived from Monte Carlo experiments, the size distributions of the corresponding 2D and 3D cells. The idea that random Voronoi areas and volumes follow gamma distributions with indices 4 and 6 respectively was later referred to as "Kiang's conjecture", see Okabe et al. (1992). The application of Voronoi diagram to the distribution of galaxies started with Icke & van de Weygaert (1987), using initial seeds generated by a sequential clustering process. Later on Pierre (1990) introduced a general algorithm for simulating one-dimensional lines of sight through a cellular universe. The large microwave background temperature anisotropies over angular scales up to one degree were calculated using a Voronoi model for large-scale structure formation in Barrow & Coles (1990) and Coles (1991).

The possibility to explain the CfA slices using a fractal distribution of seeds and inserting the galaxies on the faces of the irregular polyhedron was explored by Zaninetti (1991). A detailed Monte Carlo simulation of pencil beam-like redshift surveys was carried out by Subba Rao & Szalay (1992): they found that the probability of finding regularity varies from 3 to 15 percent depending on the details of the models. Another Monte Carlo study was carried out by van de Weygaert & Babul (1994) where three different distributions of nuclei were adopted in order to perform extensive statistical analysis of several geometrical aspects of three dimensional Voronoi tessellation. In a different context, a new way of partitioning space into cells the shape of rhombic dodecahedron was introduced in Kiang (2003); and applications were made to the CfA catalogue and to the IRAS/PSCz catalogue (Kiang et al. 2004). A void hierarchy approach was introduced in Sheth & van de Weygaert (2004) which contains two parameters characterising respectively the dynamics of the formation of voids and collapsed objects.

We now briefly review some published astronomical observations that point to a cellular structure of the universe. On analysing the data from four distinct surveys at the north and south Galactic poles Broadhurst et al. (1990) found an apparent regularity in the galaxy distribution with a characteristic scale of 128 Mpc. The astronomers that analysed the maps of the galaxy distribution up to cz=15 000 km s $^{-1}$ (see for example de Lapparent et al. (1988) and Geller & Huchra (1989)) found large coherent structures: the largest void found having a diameter of 5000 km s $^{-1}$. Great advances in the observational data (see Folkes et al. 1999; Ratcliffe et al. 1996 and Shectman et al. 1996), brought the limits of the observations to cz=60 000 km s $^{-1}$ and confirmed the existence of voids in the distribution of galaxies. The distribution of clusters in rich superclusters is not isotropic: it is periodic along a cubic lattice approximately aligned with the super-galactic coordinates, see for example Saar et al. (2002).

The Voronoi diagrams are also used to process the astronomical data, see El-Ad & Piran (1997) and Ramella et al. (2001). As an example Ramella et al. (2001) implemented a Voronoi Galaxy Cluster Finder that uses galaxy positions and magnitudes to find clusters and determine their main features: size, richness and contrast above the background.

One possible starting point is to consider a series of explosions that took place at the same time in a homogeneous space. The shells from the explosions meet in a 3D network of irregular polyhedra. From an astrophysical point of view this network can be realized by a set of primordial explosions, see Charlton & Schramm (1986) and Zaninetti & Ferraro (1990), described by the Sedov solution in the adiabatic phase:

$$R(t) = \left(\frac{25}{4}\,\frac{E\,t^2}{\pi\,\rho}\right)^{1/5} = 12.49\,\mathrm{Mpc}\left(\frac{E_{64}\;{t_9}^2}{n_{-7}}\right)^{1/5}, \tag{1}$$

where t represents the time, E the energy injected in the explosion, ρ the density of matter, $\rho = n\mathrm{m}$, n the number of particles per unit volume, $m = 1.4 m_{\mathrm{H}}$, m_{H} the mass of the hydrogen, $t_9 = t/10^9$ yr, $E_{64} = E/10^{64}$ erg and $n_{-7} = n/(10^{-7}\mathrm{particles\,cm^{-3}})$.

The above cited works leave the following questions unanswered or only partially answered. Is "Kiang's conjecture" applicable to the distribution of the galaxies? What is the probability density function of a two–dimensional section of a 3D Voronoi network? Can the averaged area connected with the voids in the distribution of galaxies visible on the CfA2 slices be guessed from the theory? Can the number of theoretical voids in the distribution of galaxies in a sphere of radius equal to that of the CfA2 slices be deduced theoretically?

One way of answering these questions is to derive the index of the gamma distribution that characterises the distribution of the 2D and 3D Voronoi cells, see Sections 2.5 and 3.3. The index of the gamma distribution that characterises the sectional area of a 3D Voronoi network as well some characteristics of the voids in the distribution of galaxies will be derived in Section 3.1. The observed large scale structures of galaxies are referred to as CfA slices, LCRS slices or pencil beam surveys: they are simulated in Section 4. The number of seeds necessary to produce a theoretical network comparable to the observed one is computed in Section 4.1.1.

2 THE PRELIMINARIES

The type of adopted lattice, the importance of setting properly the boundary conditions, the type of seeds that generates the polygons/polyhedron, the concept of unitarian area and volume and a first two dimensional scan are now introduced.

2.1 The Adopted Lattice

We start with a 2D or a 3D lattice made of pixels^2 and pixels^3 points: present in this lattice are N_s seeds generated according to some random process. All the computations are usually performed on this mathematical lattice; the conversion to the physical lattice is obtained by multiplying the unit by $\delta = \frac{\mathrm{side}}{\mathrm{pixels}-1}$, where 'side' is the length of the square/cube expressed in the adopted physical units.

2.2 Boundary Conditions

In order to minimise boundary effects introduced by those polygons/polyhedra that cross the lattice boundary, we amplify the area/cube in which the seeds are inserted by a factor 'amplify'. Therefore the N seeds are inserted in an area/volume that is $\mathrm{pixels}^2 \times \mathrm{amplify}$ or $\mathrm{pixels}^3 \times \mathrm{amplify}$, which is bigger than the box over which we perform the scanning; 'amplify' is generally taken to be equal to 1.2. This procedure inserts periodic boundary conditions to our square/cube. The number of seeds that fall in the area/cube is N_s with $N_s < N$. In order to avoid computing incomplete area/volumes we select the cells that do not intersect the square/cubic boundary. This is obtained by selecting the cells that belong to seeds that are contained in an area/volume that is 'select' times smaller than pixels^2 or pixels^3; 'select' is taken to vary between 0.1 and 0.5.

2.3 The Seeds

The seeds are generated independently on the X and Y axis in 2D (and the Z axis in 3D) through a subroutine that returns a pseudo-random real number taken from a uniform distribution between 0 and 1. In practice we used the subroutine RAN1 as described in Press et al. (1992).

2.4 The Adopted Units

In order to deal with quantities of the order of one we divide the obtained area/volume in units of $\mathrm{pixels}^2/\mathrm{pixels}^3$ by the expected "unitarian" area/volume , u_A and u_V defined as

$$u_A = \mathrm{pixels}^2 \times \mathrm{amplify}/N\,, \tag{2}$$

$$u_V = \mathrm{pixels}^3 \times \mathrm{amplify}/N\,. \tag{3}$$

This operation represents a first normalisation. The expected unitarian quantities can also be expressed in physical units, u_A^p and u_V^p,

$$u_A^p = \mathrm{side}^2 \times \mathrm{amplify}/N\,, \tag{4}$$

$$u_V^p = \mathrm{side}^3 \times \mathrm{amplify}/N\,. \tag{5}$$

Special attention should be paid when we deal with a 2D cut of a 3D network; this case is named $V_p(2,3)$, see Section 3.1. The unitarian area $u_{A(2,3)}$ is expected to be

$$u_{A(2,3)} = u_V^{2/3}\,, \tag{6}$$

and the physical counterpart

$$u^p_{A(2,3)} = (u_V^p)^{2/3}\,. \tag{7}$$

2.5 The Two Dimensional Scan

A lattice made of $(\mathrm{pixel})^2$ points is considered and a typical run using the seeds as given by a random process is presented in Figure 1. Once the histogram of the area is obtained, we can fit it, following Kiang (1966), with the following one parameter probability density function (pdf):

$$H(x;c) = \frac{c}{\Gamma(c)}(cx)^{c-1}\exp(-cx)\,, \tag{8}$$

where $0 \leq x < \infty$, $c > 0$ and $\Gamma(c)$ is the gamma function with argument c. This pdf is characterised by μ=1 and σ^2=1/c. The value of c is obtained from the method of the matching moments,

$$c = \frac{1}{\sigma^2} = \frac{n-1}{\sum_{i=1}^{n}(x_i-1)^2}\,. \tag{9}$$

The data should be normalised in order to have $\overline{x} = 1$. The frequency histogram and its best fit with the gamma-variate are shown in Figure 2. The caption of Figure 2 includes also the following quantities

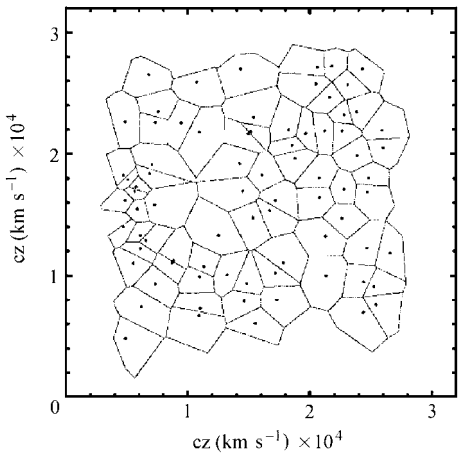

Fig. 1 The 2D Voronoi–diagram defined by random seeds. The parameters are pixels $= 800$, $N = 180$, amplify $= 1.2$, side $= 2 \times 16\,000$ km s^{-1} and select $= 0.5$.

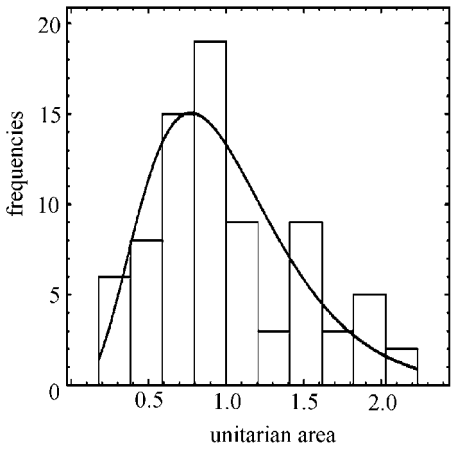

Fig. 2 Histogram of area size and the best fitting gamma distribution; same input parameters as in Figure 1, $c = 4.38$, number of bins =10 , $\chi^2 = 12.67$, $\overline{A} = 0.98$, $A_{\max} = 2.19$ and $A_{\min} = 0.17$.

expressed in normalised area units (see formula (3)) $\overline{A}$, $A_{\max}$ and $A_{\min}$, respectively the averaged, the maximum and the minimum of the area–sample and χ^2, that represents the goodness of fit.

The value of c in the case of 2D random Voronoi cells according to "Kiang's conjecture" is $c = 4$; in this numerical simulation, we have $c = 4.38$.

3 THE 3D CASE

In order to make a comparison with the astronomical observations the tessellation in $\Re^3$ is firstly analysed through a planar section and the distribution of volume is numerically derived.

3.1 The 2D Cut

We now work on a 3D lattice $L_{k,m,n}$ of pixels^3 elements. Given a section of the cube (characterised, for example, by $k = \frac{\text{pixel}}{2}$) the various V_i (the volume belonging to the seed i) may or may not cross the little cubes belonging to the two dimensional lattice.

Following the nomenclature introduced by Okabe et al. (1992) we can call the intersection between a plane and the cube previously described as $V_p(2,3)$. A typical result of this 2D sectional operation in the x-y plane is presented in Figure 3, the frequency histogram and the best fit with a gamma-variate pdf of the $V_p(2,3)$ distribution are shown in Figure 4 together with the derived value of c. We assume that galaxies are distributed on the faces of the irregular polyhedra so we expect to find concentrations of galaxies along the boundaries shown in Figure 3. The thick edges of Figure 3 represent the intersection between the "observed slice" and a face.

Considering the great importance of the $V_p(2,3)$ diagram in the astrophysical applications we considered three such diagrams in the x-y, x-z and y-z planes. This allowed us to find the average values of the sample properties and their errors, given in the captions of Figure 4.

The mathematical theory of the cell size distribution in 1D Poisson Voronoi diagram, see Okabe et al. (1992), gives

$$\overline{A} = 0.68\lambda^{-2/3}\,, \tag{10}$$

where λ is the intensity of the Poisson process. Our values of $\overline{A}$, see captions in Figure 4, are near to the values predicted by the mathematical theory. The frequency distribution of the number of edges/crossed faces is shown in Table 1 together with the theoretical values given in Okabe et al. (1992).

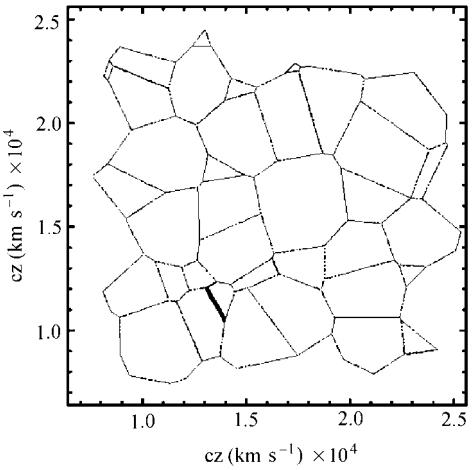

Fig. 3 A $V_p(2,3)$ diagram generated by random seeds. The parameters are pixels $= 800$, $N = 1900$, side $= 2 \times 16\,000$ km s^{-1}, amplify $= 1.2$ and select $= 0.1$.

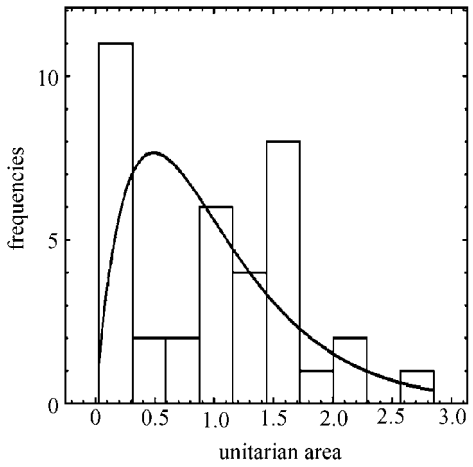

Fig. 4 Histogram of the area distribution of the $V_p(2,3)$ diagram of Fig. 3. Shown also is the best fit gamma distribution. The parameters are $c = 1.99 \pm 0.22$, number of bin =10, χ^2=23.09, $\overline{A}$ = 0.78 $\pm$ 0.06, $A_{\max} = 2.12 \pm 0.26$ and $A_{\min}$ = 0.02$\pm$ 0.01.

Table 1 The Probability to have n–edges in $V_p(2,3)$

seeds $\setminus$ n	3	4	5	6	7	8	9
Okabe et al. (1992)	0.063	0.13	0.2	0.22	0.18	0.11	0.05
random	0.081	0.16	0.24	0.18	0.10	0.16	0.054

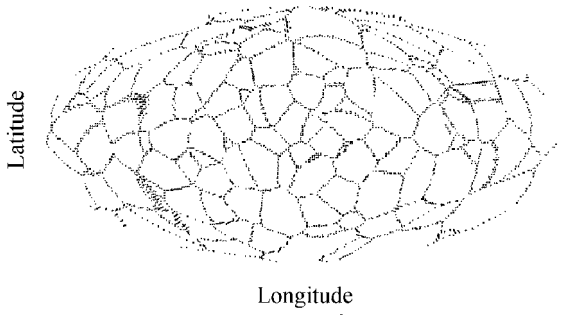

Fig. 5 Voronoi–diagram $V_p(2,3)$ in the Hammer-Aitof projection at cz = 7201 km s^{-1}.

The derived values of c recall the theoretical distribution of 1D Voronoi segments in which $c = 2$, see Kiang (1966) .

3.2 Projection on the Sphere

Another type of a 2D section of a 3D Voronoi network is a spherical cut defined by a constant value of the distance to the center of the box. One such section is shown in Figure 5.

3.3 The Statistics of the Volume

For every lattice point $L_{k,m,n}$ we compute the nearest seed and we increase by one the volume "belonging to" that seed. The frequency histogram and the relative best fit through gamma-variate pdf for the volume distribution is reported in Figure 6.

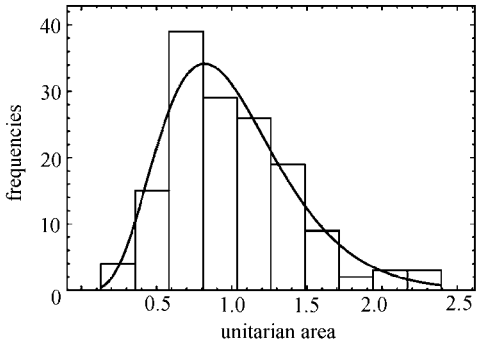

Fig. 6 Histogram of the 3D Voronoi volumes. Also shown is the best-fit gamma distribution. The parameters are pixels = 400, $c = 5.50$, NBIN=10 and χ^2=8.05.

The experimental frequencies are fitted by a gamma–variate with $c = 5.5$. This value of c should be compared with the value of 6 which was first conjectured by Kiang (1966) but later refined to 5.5 (Kiang 1990) and with the value of 5.78 deduced by Kumar et al. (1992).

4 THE SPATIAL DISTRIBUTION OF GALAXIES

The theory of the sectional area derived in Section 3.1 can be the framework that interprets the existence of voids in the spatial distribution of galaxies. The observational evidence for the voids is briefly reviewed and then the number of voids in the distribution of galaxies of the CfA2 slices is derived. We shall calibrate our Voronoi diagrams with the largest observed void size in the CfA slices in our simulation of the observed galaxy distribution.

4.1 The CfA2 Slices

The second CfA2 redshift Survey, started in 1984, showed that the spatial distribution of galaxies is not random but tends to concentrate in filaments that could be interpreted as 2D projections of 3D bubbles. We recall that a "slice" in the survey comprises all the galaxies with magnitude $m_b \leq 16.5$ in a strip of 6° wide and about 130° long. One such slice (the so called first CfA strip) is available at the address http://cfa-www.harvard.edu/ huchra/zcat/; more details can be found in Geller & Huchra (1989). This slice can be down-loaded from http://cfa-www.harvard.edu/ huchra/zcat/n30.dat/.

The first of such slices presents many voids, the bigger one being 4000÷5000 km s $^{-1}$ across (Huchra 2003). The greatest possible attention should be paid to the derivation of the largest void area, $A^{\rm obs}_{\rm max}$, because this is the area that fixes the scale of the voids in the simulated distribution of galaxies.

The average value of voids diameter can be derived from the following proportion:

$$\frac{A_{\rm max}}{\overline{A}} = \frac{A^{\rm obs}_{\rm max}}{\overline{A}^{\rm obs}}\,, \tag{11}$$

where the left hand side refers to the maximum and average value of the simulated cross-sectional area $V_p(2,3)$ (their numerical values are visible in the captions of Figure 2) and the right hand side refers to the same quantities on the CfA2 slices. A value for the average observed diameter, $\overline{D^{\rm obs}}$, is easily found from the previous proportion:

$$\overline{D^{\rm obs}} \approx 0.6 D^{\rm obs}_{\rm max} = 2700\,{\rm km\,s^{-1}} = 27\,{\rm Mpc}\,, \tag{12}$$

where $D^{\rm obs}_{\rm max} = 4500\,{\rm km\,s^{-1}}$ corresponds to the extension of the maximum void visible on the CfA2 slices. The half value of $\overline{D^{\rm obs}}$ can be equated with Equation (1) that gives the radius of the explosion from primeval galaxies and the following is obtained:

$$\frac{E_{64}\ {t_9}^2}{n_{-\gamma}} = 1.47\,. \tag{13}$$

This relationship regulates the three basic physical parameters involved in the explosions of primeval galaxies. The results of the simulation can be represented by a slice similar to that observed (a strip of 6° wide and about 130° long), see Figure 7.

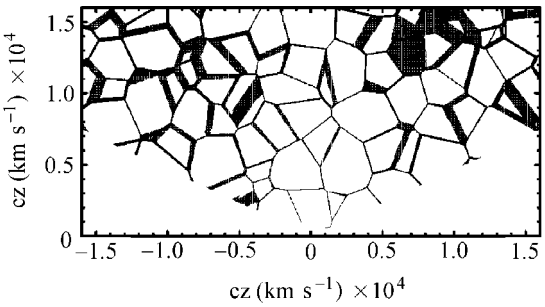

Fig. 7 Polar plot of Voronoi cells belonging to a slice 130° long and 6° wide. Same parameters as in Figure 3.

For a more accurate confrontation between simulation and observations the effect due to the distribution in luminosity should be introduced. Here we simply adopt the following "scaling" algorithm:

1. The field of velocity of the observed sample is divided in NBIN intervals equally spaced.
2. In each of these NBIN intervals the number of galaxies NGAL(j) (j identifies the selected interval) is computed.
3. The field of velocity of the simulated cells belonging to the faces is sampled as in point (1).
4. In each interval of the simulated field of velocity NGAL(j) elements are randomly selected.
5. At the end of this process the number of cells belonging to the faces equalises the number and the scaling of the observed galaxies.

A typical polar plot after the "scaling" algorithm is implemented is shown in Figure 8; its general appearance should be compared with that of the observed plot, see Figure 9.

4.1.1 The density of voids

The density of seeds expressed in physical units, ρ_N, is the inverse of the physical averaged volume, $\rho_N = 1/u^p_V$, and therefore

$$u^p_{A(2,3)} = (u^p_V)^{2/3} = \Big(\frac{1}{\rho_N}\Big)^{2/3}. \tag{14}$$

At the same time the sectional area will be characterised by a maximum physical area, $A^{\,p}_{\rm max}$, expressed in physical units,

$$A^p_{\rm max} = C_{\rm Amax} \times u^p_{A(2,3)}\,, \tag{15}$$

and the following is easily found

$$\rho_N = \Big(\frac{C_{\rm Amax}}{A^p_{\rm max}}\Big)^{3/2}. \tag{16}$$

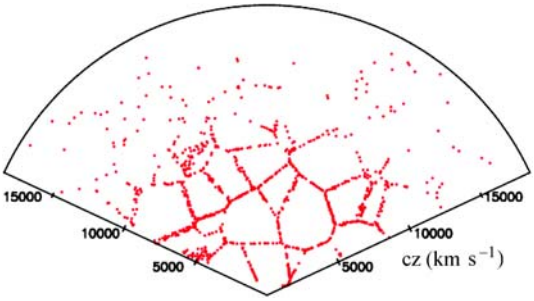

Fig. 8 A Polar plot of the simulated galaxies when the "scaling" algorithm is applied. NBIN=15 and other parameters as in Figure 7 .

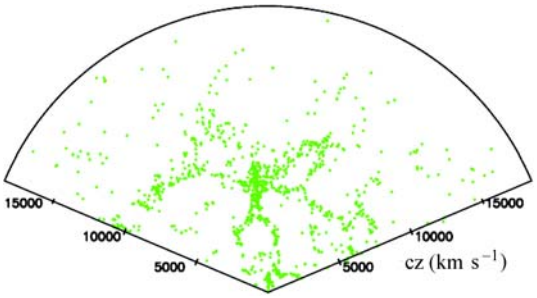

Fig. 9 Polar plot of the real galaxies belonging to the second CfA2 redshift catalogue.

We are now ready to compute the number of sources in a sphere of radius $R_{\rm obs} = 16\,000\,{\rm km\ s^{-1}}$, the same radius that characterises the CfA2 slices. The number of voids/seeds in the sphere turns out to be

$$N = \frac{1.7 \times 10^{13} (C_{\rm Amax})^{3/2}}{(A^{\rm obs}_{\rm max})^{3/2}}\,, \tag{17}$$

where $A^{p}_{\rm max}$ was identified with $A^{\rm obs}_{\rm max}$. Inserting the dimension of the maximum void as deduced in Section 4.1, we obtain $A^{\rm obs}_{\rm max} = 1.59 \times 10^{7} ({\rm km\ s^{-1}})^2$. We now have an expression for the number of seeds in the sphere that characterises the CfA2,

$$N = 268 (C_{\rm Amax})^{3/2} = 827\,. \tag{18}$$

5 CONCLUSIONS

The Voronoi diagram offers one way of interpreting the voids in the observed distribution of galaxies in space. The characteristics of the cells in a two–dimensional section of a 3D Voronoi network can be compared with those of the voids in the distribution of galaxies. The following items turn out to be useful to the astronomer once $A^{\rm obs}_{\rm max}$, the maximum area connected with a void, is derived from the astronomical observations:

- The averaged value of the voids in the distribution of galaxies should be 2741 ± 210 km s $^{-1}$ across.
- The pdf of the area of the voids in the distribution of galaxies should be a gamma–variate with index 1.9.
- The expected averaged value of the sides of the irregular polygons that characterises the voids in the distribution of galaxies should be 5.

The following are some further points to investigate:

- The maximum area connected with a void should be derived with a great accuracy in the various slices.
- The algorithms of describing polygonal voids from the astronomical observations should be developed in order to test the suggested averaged number of sides, 5, as predicted from the Voronoi diagrams.
- The pdf of the area connected with the voids should be tentatively computed in order to test the predictions of the $V_p(2,3)$ diagrams.

The Voronoi diagrams allow also to reformulate the theory of the primordial explosions because

- The average diameter of voids between galaxies is function of three parameters: time, density and energy, see Equation (13).
- The galaxies are supposed to originate where the primordial shells meet, the faces of the Voronoi polyhedra.
- The correlation length for galaxies can be identified with the face's thickness that is approximately 1/6 the radius of the expanding shell.

Acknowledgements I thank the Smithsonian Astrophysical Observatory and John Huchra for the small catalog available from the web at *http://cfa-www.harvard.edu/ huchra/zcat/*. I thank the referee for useful suggestions.

References

Barrow J. D., Coles P., 1990, MNRAS, 244, 188
Broadhurst T. J., Ellis R. S., Koo D. C., Szalay A. S. 1990, Nature, 343, 726
Charlton J. C., Schramm D. N., 1986, ApJ, 310, 26
Coles P., 1991, Nature, 349, 288
de Lapparent V., Geller M. J., Huchra J. P., 1988, ApJ, 332, 44
El-Ad H., Piran T., 1997, ApJ, 491, 421
Folkes S., Ronen S., Price I. et al., 1999, MNRAS, 308, 459
Geller M. J., Huchra J. P., 1989, Science, 246, 897
Huchra J. P., 2003, private communication
Icke V., van de Weygaert R., 1987, A&A, 184, 16
Kiang T., 1966, Zeitschrift fur Astrophysics, 64, 433
Kiang T., 1990, private communication
Kiang T., 2003, ChJAA, 3, 95
Kiang T., Wu Y.-F., Zhu X.-F., 2004, ChJAA, 4, 209
Kumar S., Kurtz S. K., Banavar J. R., M. G. S., 1992, Journal of Statistical Physics, 67, 523
Okabe A., Boots B., Sugihara K., 1992, Spatial tessellations. Concepts and Applications of Voronoi diagrams (Chichester, New York: Wiley)
Pierre M., 1990, A&A, 229, 7
Press W. H., Teukolsky S. A., Vetterling W. T., Flannery B. P., 1992, Numerical recipes in FORTRAN. The art of scientific computing, Cambridge: Cambridge University Press
Ramella M., Boschin W., Fadda D., Nonino M., 2001, A&A, 368, 776
Ratcliffe A., Shanks T., Broadbent A. et al., 1996, MNRAS, 281, L47+
Saar E., Einasto J., Toomet O. et al., 2002, A&A, 393, 1
Shectman S. A., Landy S. D., Oemler A. et al., 1996, ApJ, 470, 172
Sheth R. K., van de Weygaert R., 2004, MNRAS, 350, 517
Subba Rao M. U., Szalay A. S., 1992, ApJ, 391, 483
van de Weygaert R., Babul A., 1994, ApJ, 425, L59
Voronoi G., 1908, Z. Reine Angew. Math, 134, 198
Zaninetti L., 1991, A&A, 246, 291
Zaninetti L., Ferraro M., 1990, A&A, 239, 1